

Supporting Information

Construct $\text{Mn}_x\text{Co}_y\text{O}_4/\text{Ti}$ Electrocatalysts for Efficient Bifunctional Water Splitting

Qiuping Huang,^{a#} Mingjiao Jiang,^{b#} Yingjia Li,^b Chao Liang,^b Yumei Tang,^b Fengyu Xie,^a Min Yang,^{b*} Guowei Deng,^{b*}

a. College of Chemistry and Materials Science Sichuan Normal University, Chengdu, Sichuan 610066, China

b. College of Chemistry and Life Science, Sichuan Provincial Key Laboratory for Structural Optimization and Application of Functional Molecules, Chengdu Normal University, Chengdu 611130, China

Number of pages: 25

Number of figures: 15

Number of tables: 5

Content

XRD patter of $Mn_xCo_yO_4/Ti$	Fig. S1
Nitrogen ad-/desorption isotherms of $Mn_xCo_yO_4/Ti$ (Mn:Co=1:2).....	Fig. S2
SEM images of $Mn_xCo_yO_4/Ti$ thin film (a), Ti mesh surface (b), $Mn_xCo_yO_4$ presented a uniform micro-flower (c), The micro-flower was found to be composed of nanosheets (d) ...	Fig. S3
SEM images of $Mn_xCo_yO_4/Ti$ (Mn:Co=2:1) (a,b) and $Mn_xCo_yO_4/Ti$ (Mn:Co=1:1) (c,d).....	Fig. S4
SEM of the film on Ti mesh at low (a, b) and high magnification (c, d).....	Fig. S5
Fitted O 1s XPS spectra of $Mn_xCo_yO_4/Ti$ (Mn:Co=1:2).....	Fig. S6
The different ratio of $Mn_xCo_yO_4$ on Ni foam.....	Fig. S7
Cyclic voltammetry curves of $Mn_xCo_yO_4/Ti$	Fig. S8
$Mn_xCo_yO_4/Ti$ Electrocatalyst for ECSA.....	Fig. S9
Cyclic voltammetry curves of $Mn_xCo_yO_4/Ti$ in Faradic region.....	Fig. S10
TOF of $Mn_xCo_yO_4/Ti$ for HER.....	Fig. S11
TOF of $Mn_xCo_yO_4/Ti$ for OER.....	Fig. S12
The multi-current process of $Mn_xCo_yO_4/Ti$ (Mn:Co=1:2) for OER.....	Fig. S13
Raman of the $Mn_xCo_yO_4/Ti$ (Mn:Co=1:2) after long cycling tests.....	Fig. S14
XPS of the $Mn_xCo_yO_4/Ti$ (Mn:Co=1:2) after long cycling tests.....	Fig. S15
Comparison of HER performance.....	Table S1
Comparison of OER performance.....	Table S2
Comparison of overall spiltting water performances performance.....	Table S3
HER-TOF determined at 300 mV (vs RHE).....	Table S4
OER-TOF determined at 300 mV (vs RHE).....	Table S5

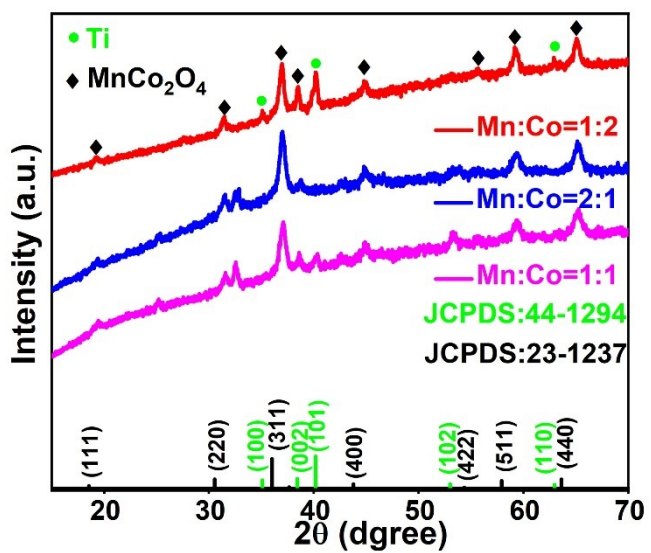


Fig. S1. XRD pattern of Mn_xCo_yO₄/Ti.

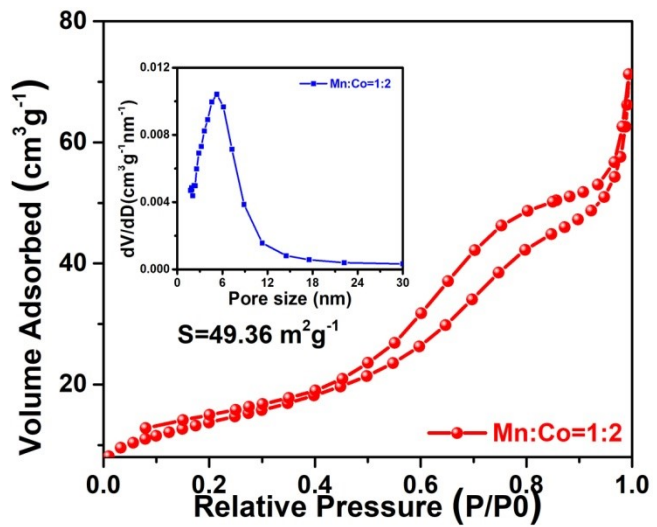


Fig. S2. Nitrogen ad-/desorption isotherms and pore size distribution of $\text{Mn}_x\text{Co}_y\text{O}_4/\text{Ti}$ (Mn:Co=1:2).

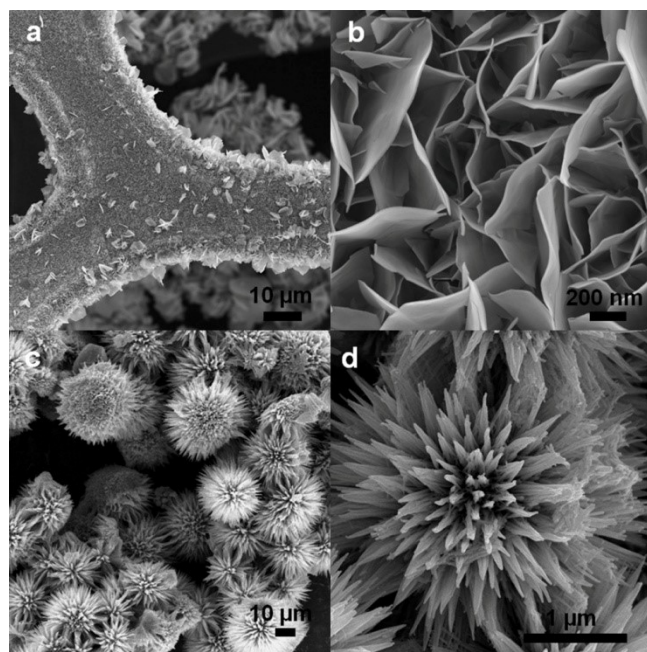


Fig. S3. SEM images of Mn_xCo_yO₄/Ti thin film (a), Ti mesh surface (b), Mn_xCo_yO₄/Ti (Mn:Co=1:2) presented a uniform micro-flower (c), The micro-flower was found to be composed of nanosheets (d)

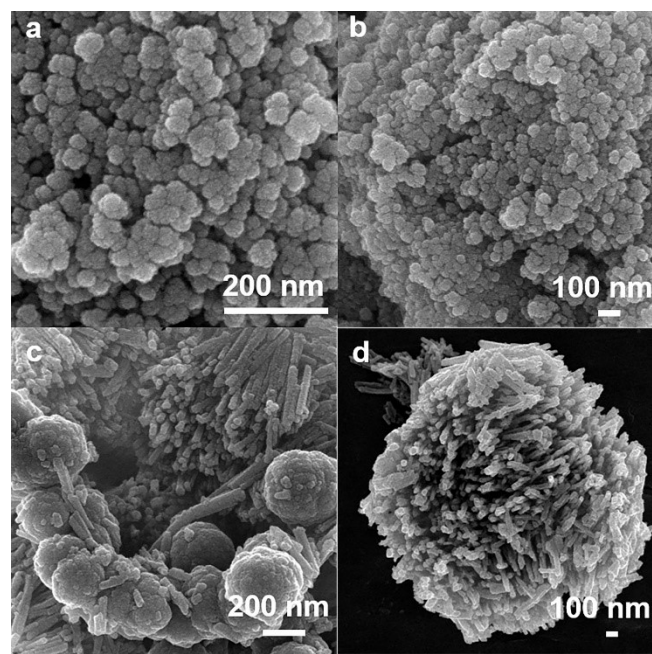


Fig. S4. SEM images of Mn_xCo_yO₄/Ti (Mn:Co=2:1) (a, b) and Mn_xCo_yO₄/Ti (Mn:Co=1:1) (c, d).

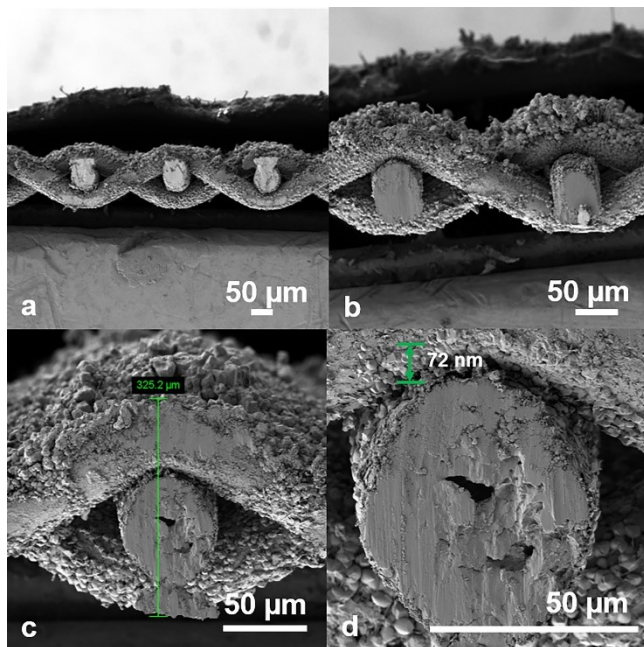


Fig. S5. SEM of the film on Ti mesh at low (a, b) and high magnification (c, d).

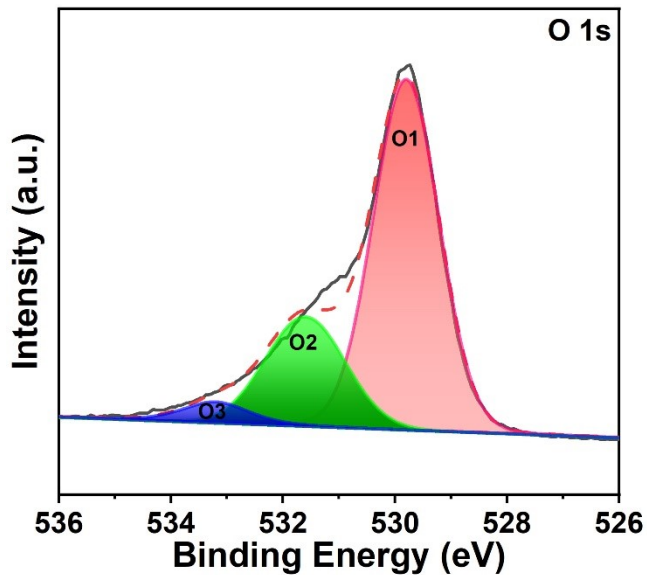


Fig. S6. Fitted O 1s XPS spectra of $\text{Mn}_x\text{Co}_y\text{O}_4/\text{Ti}$ (Mn:Co=1:2).

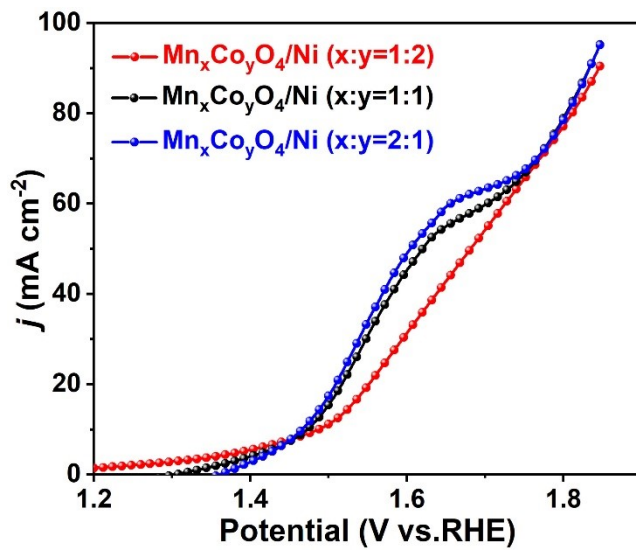


Fig. S7. The different ratio of $\text{Mn}_x\text{Co}_y\text{O}_4$ on Ni foam.

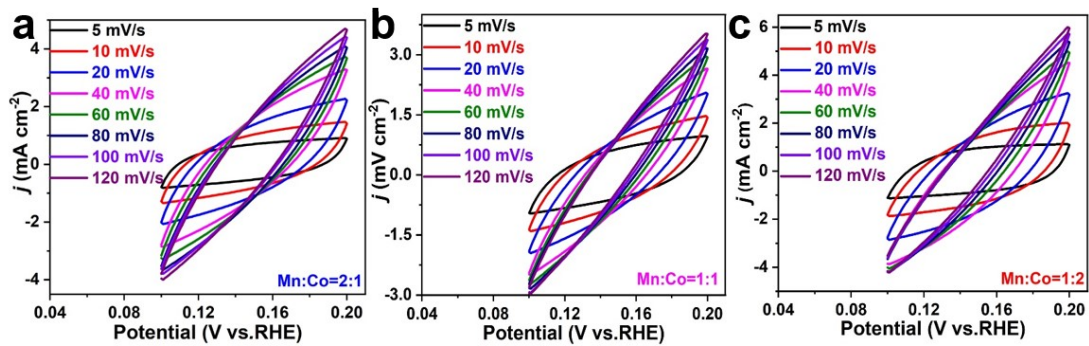


Fig. S8. Cyclic voltammograms of $\text{Mn}_x\text{Co}_y\text{O}_4/\text{Ti}$ (Mn:Co=2:1), $\text{Mn}_x\text{Co}_y\text{O}_4/\text{Ti}$ (Mn:Co=1:1), $\text{Mn}_x\text{Co}_y\text{O}_4/\text{Ti}$ (Mn:Co=1:2) electrode in the non-Faradaic current range at scan rates of 5,10,20, 40, 60, 80 , 100 mV s^{-1} and 120 mV s^{-1} for ECSA.

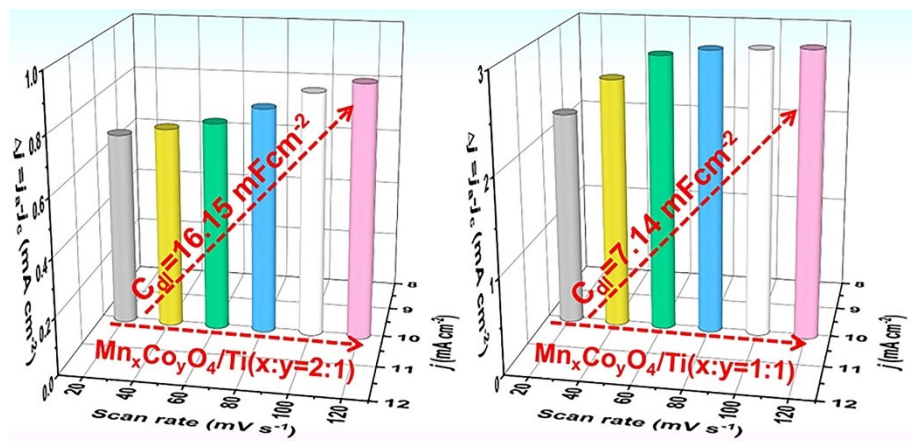


Fig. S9. C_{dl} calculation of Mn_xCo_yO₄/Ti (Mn:Co=1:1) (a) and C_{dl} calculation of Mn_xCo_yO₄/Ti (Mn:Co=2:1) (b).

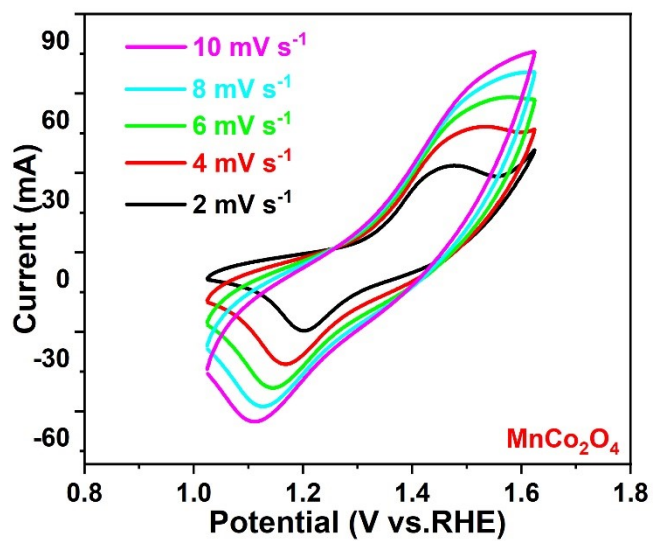


Fig. S10. Electrochemical cyclic voltammetry curves of $\text{Mn}_{\text{x}}\text{Co}_{\text{y}}\text{O}_4/\text{Ti}$ (Mn:Co=1:2) at different scanning rates in Faradic region.

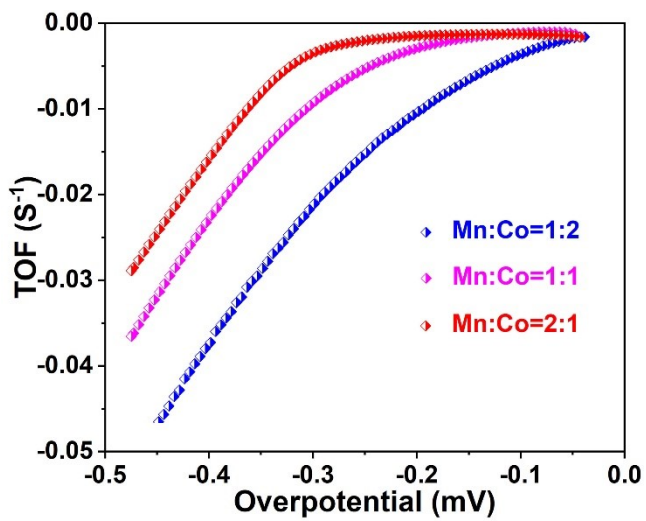


Fig. S11. The relationships between turnover frequencies and overpotentials of $Mn_xCo_yO_4/Ti$ for HER.

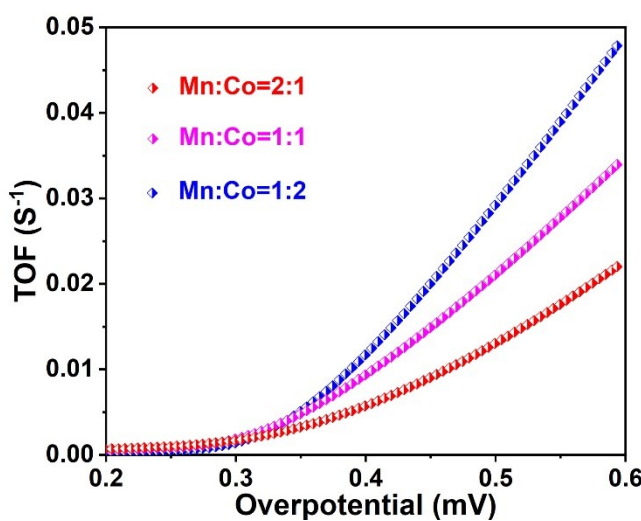


Fig. S12. The relationships between turnover frequencies and overpotentials of $\text{Mn}_x\text{Co}_y\text{O}_4/\text{Ti}$ for OER.

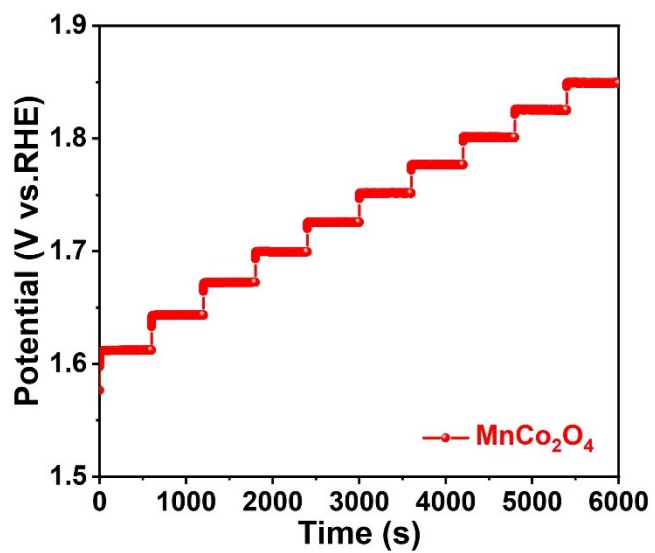


Fig. S13. The multi-current process of Mn_xCo_yO₄/Ti (Mn:Co=1:2) for OER.

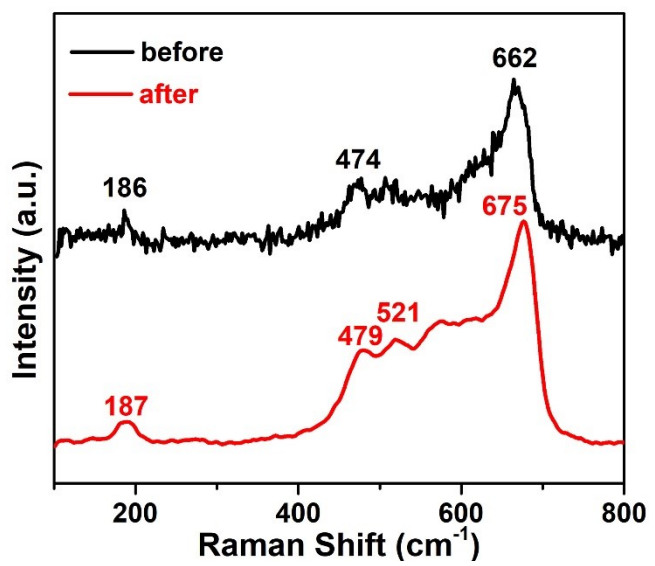


Fig. S14. Raman of the $\text{Mn}_x\text{Co}_y\text{O}_4/\text{Ti}$ ($\text{Mn}:\text{Co}=1:2$) after long cycling tests.

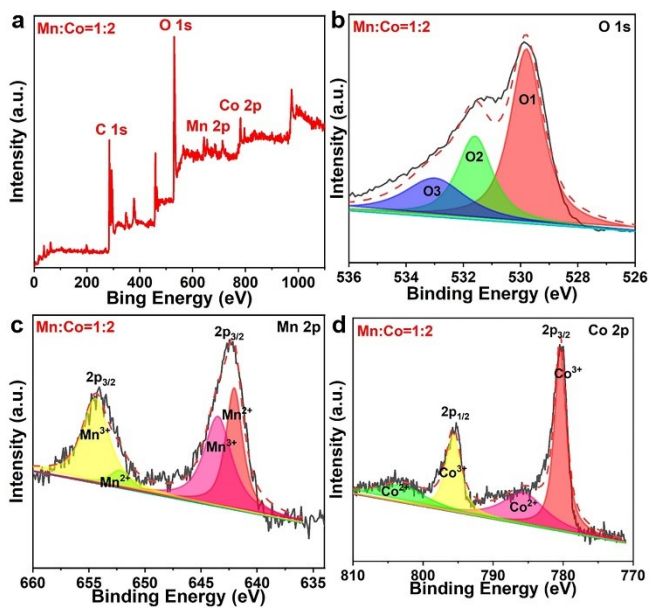


Fig. S15. XPS of the $\text{Mn}_x\text{Co}_y\text{O}_4/\text{Ti}$ ($\text{Mn}:\text{Co}=1:2$) after long cycling tests.

Table S1. The HER performances of the as-prepared MnCo₂O₄/Ti electrode and other electrodes with electrocatalysts in 1.0 M KOH.

Catalyst	Electrolyte	j (mAcm ⁻²)	η (mV)	Tafel (mV·dec ⁻¹)	Ref.
MnCo₂O₄/Ti	1M KOH	10	168	174	This work
NiCo ₂ O ₄ /Cu	1M KOH	10	295	210	[1]
NiFeOP	1M KOH	10	209	161	[2]
Ni _{0.09} Co _{2.91} O ₄ /Ti ₃ C ₂ T _x -HT	1M KOH	10	210	106	[3]
CoP/CNFs	1M KOH	10	225	100	[4]
Co _x P@Co ₃ O ₄	1M KOH	10	106	16	[5]
CoS/NiOOH	1M KOH	10	170	120	[6]
NCS	1M KOH	10	231	92	[7]
Co/CoP	1M KOH	10	151	70	[8]
NiCoFeMnCrP NPs	1M KOH	10	220	94	[9]

References

- [1] Ouyang, Q.; Lei, Z., Li, Q.; Li, M., Yang, C., H. A self-supported NiCo₂O₄/Cu_xO nanoforest with electronically modulated interfaces as an efficient electrocatalyst for overall water splitting. *J. Mater. Chem. A.* 2021, 9, 14466–14476.
- [2] Chen, J., S.; Guo, Z., Z.; Luo, Y., X.; Cai, M., D.; Gong, Y., X.; Sun, S.; Li, Z., X.; Mao, C., J. Engineering Amorphous Nickel Iron Oxyphosphide as a Highly Efficient Electrocatalyst toward Overall Water Splitting. *ACS Sustainable Chem. Eng.* 2021, 9, 9436–9443.
- [3] Xu, P., W.; Wang, H., H.; Liu, J.; Feng, X., Z.; Ji, W., J.; Au, C., T. High-Performance NixCo_{3-x}O₄/Ti₃C₂T_x-HT Interfacial Nanohybrid for Electrochemical Overall Water Splitting. *ACS Appl. Mater. Interfaces*, 2021, 13, 34308–34319.
- [4] Xie, X., Q.; Liu, J., P.; Gu, C., N.; Li, J., J.; Zhao, Y.; Liu, C., S. Hierarchical structured CoP nanosheets/carbon nanofibers bifunctional electrocatalyst for high-efficient overall water splitting. *Journal of Energy Chemistry*, 2022, 64, 503-510.

- [5] Xu, X, H.; Wang, T.; Lu, W, B.; Dong, L, j.; Zhang, H, S.; Miao, X, Y. Co_xP@Co₃O₄ Nanocomposite on Cobalt Foam as Efficient Bifunctional Electrocatalysts for Hydrazine-Assisted Hydrogen Production. ACS Sustainable Chem. Eng, 2021, 9, 4688–4701.
- [6] Wu, H,; Lu, Q,; Zhang, J, F,; Wang, J, J,; Han, X, P,; Zhao, N, Q,; Hu, W, B,; Li, J, J,; Chen, Y, N,; Deng, Y, D. Thermal Shock-Activated Spontaneous Growing of Nanosheets for Overall Water Splitting. Nano-Micro Lett. 2020, 162,2-12.
- [7] Li, H, Q,; Chen, L,; Jin, P, F,; Li, Y, F,; Pang, J, X,; Hou, J,; Peng, S, L,; Wang, G,; Shi, Y, L. NiCo₂S₄ microspheres grown on N, S co-doped reduced graphene oxide as an efficient bifunctional electrocatalyst for overall water splitting in alkaline and neutral PH. Nano Research. 2022, 15, 950-958.
- [8] Zhang, Y, Y,; Qiu, Y, F,; Ma, Z,; Wang, Y, P,; Zhang, Y, X,; Ying, Y, X,; Jiang, Y, N,; Zhu, Y, X,; Liu, S, Q. Core-corona Co/CoP clusters strung on carbon nanotubes as a Schottky catalyst for glucose oxidation assisted H₂ production. J. Mater. Chem. A, 2021, 9, 10893-10908.
- [9] Lai, D, W,; Kang, Q, L,; Gao, F,; Lu, Q, Y. High-entropy effect of a metal phosphide on enhanced overall water splitting performance. J. Mater. Chem. A, 2021, 9, 17913-17922.

Table S2. The OER performances of the as-prepared MnCo₂O₄/Ti electrode and other electrodes with electrocatalysts in 1.0 M KOH.

Catalyst	Electrolyte	j (mA cm ⁻²)	η (mV)	Tafel (mV·dec ⁻¹)	Ref.
MnCo ₂ O ₄ /Ti	1M KOH	10	229	92	This work
Co/Co ₂ Mo ₃ O ₈ @NC	1M KOH	10	288	86	[1]
Ni/NiP@N-CNF	1M KOH	10	285	45	[2]
MnCo ₂ O ₄	1M KOH	10	440	75	[3]
MnCo ₂ O ₄	0.1M KOH	10	400	87	[4]
CoO-Co4N@NiFe-LDH/NF	1M KOH	10	231	39	[5]
VCoCOX@NF	1M KOH	10	240	23	[6]
NiFeOP	1M KOH	10	310	43	[7]
NiFe-MOF	1M KOH	10	240	73	[8]
Ni-M@C-130	1M KOH	10	240	47	[9]

References

- [1] Zhang, Y, N.; Ye, W, L.; Fan, J, C.; Cecen, V.; Shi, P, H.; Min, Y, L.; Xu, Q, J. Cobalt-Nanoparticle-Decorated Cobalt–Molybdenum Bimetal Oxides Embedded in Flower-like N-Doped Carbon as a Durable and Efficient Electrocatalyst for Oxygen Evolution Reaction. ACS Sustainable Chem. Eng. 2021, 9, 11052–11061.
- [2] Li, X, G.; Zhou, J, H.; Liu, C.; Xu, L.; Lu, C, L.; Yang, J.; Pang, H.; Hou, W, H. Encapsulation of Janus-structured Ni/Ni₂P nanoparticles within hierarchical wrinkled N-doped carbon nanofibers: Interface engineering induces high-efficiency water oxidation. Appl. Catal., B 2021, 298, No. 120578.
- [3] Amirzhanova, A.; Akmansen, N.; Karakaya, I.; Dag, O. Mesoporous MnCo₂O₄ NiCo₂O₄ and ZnCo₂O₄ Thin-Film Electrodes as Electrocatalysts for the Oxygen Evolution Reaction in Alkaline Solutions. ACS Appl Energy Mater. 2021, 4, 2769–2785.

- [4] Zeng, K.; Li, W.; Zhou, Y.; Sun, Z, H.; Lu, X, Y.; Yan, J.; Choi, J, H.; Yang, R, Z. Multilayer hollow MnCo₂O₄ microsphere with oxygen vacancies as efficient electrocatalyst for oxygen evolution reaction. *Chemical Engineering Journal*, 2020, 8, 127831.
- [5] Chen, B, J.; Humayun, M.; Li, Y, D.; Zhang, H, M.,; Sun, H, C.; Wu, Y.; Wang, C, D. Constructing Hierarchical Fluffy CoO–Co₄N@NiFe-LDH Nanorod Arrays for Highly Effective Overall Water Splitting and Urea Electrolysis. *ACS Sustainable Chem. Eng.* 2021, 42, 9, 14180-14192.
- [6] Meena, A.; Thangavel, P.; Nissimagoudar, A, S.; Narayan Singh, A.; Jana, A.; Sol Jeong, D.; Im, H.; Kim, K, S. Bifunctional oxovanadate doped cobalt carbonate for high-efficient overall water splitting in alkaline-anion-exchange-membrane water-electrolyzer. *Chemical Engineering Journal*. 2021, 430, 133886.
- [7] Chen, J, S.; Guo, Z, Z.; Luo, Y, X.; Cai, M, D.; Gong, Y, X.; Sun, S.; Li, Z, X.; Mao, C, J. Engineering Amorphous Nickel Iron Oxyphosphide as a Highly Efficient Electrocatalyst toward Overall Water Splitting. *ACS Sustainable Chem. Eng.* 2021, 9, 9436–9443.
- [8] Zhao, H, G.; Yu, L.; Zhang, L, T.; Dai, L, M.; Yao, F, L.; Huang, Y.; Sun, J, W. Facet Engineering in Ultrathin Two-Dimensional NiFe Metal–Organic Frameworks by Coordination Modulation for Enhanced Electrocatalytic Water Oxidation. *ACS Sustainable Chem. Eng.* 2021, 9, 10892–10901.
- [9] Srinivas, K.; Chen, Y, F.; Wang, X, Q.; Wang, B.; Karpuraranjith, M, M.; Wang, W.; Su, Z.; Zhang, W, L.; Yang, D, X, Y. Constructing Ni/NiS Heteronanoparticle-Embedded Metal–Organic Framework-Derived Nanosheets for Enhanced Water-Splitting Catalysis. *ACS Sustainable Chem. Eng.* 2021, 9, 1920–1931.

Table S3. The overall splitting water performances of the as-prepared MnCo₂O₄/Ti electrode and other electrodes with electrocatalysts in 1.0 M KOH.

Catalyst	Electrolyte	j (mAcm ⁻²)	η (mV)	Ref.
MnCo₂O₄/Ti	1M KOH	10	1.6	This work
Cu-N-SC-100	0.1M KOH	10	1.68	[1]
Co _x P-Fe ₂ P	1M KOH	10	1.62	[2]
CoP/CNFs	1M KOH	10	1.65	[3]
NiCo ₂ O ₄	1M KOH	10	1.65	[4]
Ni _{0.09} Co _{2.91} O ₄ /Ti ₃ C ₂ T _x -	1M KOH	10	1.66	[5]
HT				
Ce ₁ -CoP	1.0 M KOH	10	1.65	[6]
CFP	1.0 M KOH	10	1.75	[7]
MoS ₂ /NiFe LDH	1.0 M KOH	10	1.61	[8]
NiFeOP	1.0 M KOH	10	1.69	[9]

References

- [1] Wang, M. W.; Su, K. M.; Zhang, M. I.; Du, X.; Li, Z. H. Advanced Trifunctional Electrocatalysis with Cu-, N-, S-Doped Defect-Rich Porous Carbon for Rechargeable Zn–Air Batteries and Self-Driven Water Splitting. ACS Sustainable Chem. Eng. 2021, 9, 13324–13336
- [2] Li, D.; Zhou, C. J.; Yang, R.; Xing, Y. Y.; Xu, S. J.; Jiang, D. L.; Tian, D.; Shi, W, D. Interfacial Engineering of the Co_xP–Fe₂P Heterostructure for Efficient and Robust Electrochemical Overall Water Splitting. ACS Sustainable Chem. Eng. 2021, 9, 7737–7748.
- [3] Xie, X. Q.; Liu, J. P.; Gu, C. N.; Li J, J.; Zhao, Y.; Liu, C. S. Hierarchical structured CoP nanosheets/carbon nanofibers bifunctional electrocatalyst for high-efficient overall water splitting. Journal of Energy Chemistry, 2022, 64, 503-510.
- [4] Zhang, L.; Peng, J. H.; Zhang, W.; Yuan, Y.; Peng, K. Rational introduction of

- borate and phosphate ions on NiCo₂O₄ surface for high-efficiency overall water splitting. *Journal of Power Sources*, 2021, 490, 229541.
- [5] Xu, P, W.; Wang, H, H.; Liu, J.; Feng, X, Z.; Ji, W, J.; Au, C, T. High-Performance Ni_xCo_{3-x}O₄/Ti₃C₂T_x-HT Interfacial Nanohybrid for Electrochemical Overall Water Splitting. *ACS Appl. Mater. Interfaces* 2021, 13, 34308–34319.
- [6] Li, J, J.; Zou, S, B.; Liu, X, D.; Lu, Y.; Dong, D, H. Electronically Modulated CoP by Ce Doping as a Highly Efficient Electrocatalyst for Water Splitting. *ACS Sustainable Chem. Eng.* 2020, 8, 10009–10016.
- [7] Khalate, S, A.; Kadam, S, A.; Ma, Y, R.; Kulkarni, S, B.; Parale, V, G.; Patil, U, M. Binder free cobalt iron phosphate thin films as efficient electrocatalysts for overall water splitting. *Journal of Colloid and Interface Science*, 2022, 613, 720-732.
- [8] Li, X, P.; Zheng, L, R.; Liu, S, J.; OuYang, T.; Ye, S, Y.; Liu, Z, Q. Heterostructures of NiFe LDH hierarchically assembled on MoS₂ nanosheets as high-efficiency electrocatalysts for overall water splitting. *Chinese Chemical Letters*, 2022.

Table S4. HER-TOF determined at 300 mV (vs RHE).

Electrodes	HER-TOF $(\frac{O_2/s}{surface\ site})$
Mn:Co=1:2	0.025
Mn:Co=1:1	0.012
Mn:Co=2:1	0.006

Table S5. OER-TOF determined at 300 mV (vs RHE).

Electrodes	OER-TOF $(\frac{O_2/s}{surface\ site})$
Mn:Co=1:2	0.014
Mn:Co=1:1	0.009
Mn:Co=2:1	0.005